Journal of Asian Earth Sciences 216 (2021) 104814

Contents lists available at ScienceDirect

Journal of Asian Earth Sciences

journal homepage: www.elsevier.com/locate/jseaes

Fore-arc high and basin evolution offshore northern Sumatra using high-resolution marine geophysical datasets

Dibakar Ghosal [a,*], Maruf M. Mukti [b], Satish C. Singh [c], Helene Carton [c], Ian Deighton [d]

[a] Indian Institute of Technology Kanpur, UP 208016, India
[b] Indonesian Institute of Sciences (LIPI), Bandung 40135, Indonesia
[c] Université de Paris, Institut de physique du globe de Paris, CNRS, F-75005 Paris, France
[d] TGS, Surrey KT6 4BN, United Kingdom

ARTICLE INFO

Keywords:
Backthrust
Fore-arc basin
Northern Sumatra
Aceh Basin
West Andaman Fault
Seismic

ABSTRACT

We present a morphotectonic study of the offshore northern Sumatra fore-arc high and fore-arc basin and an evolutionary model of the area based on high-resolution marine geophysical datasets. We show that the landward slope of the fore-arc high and the western edge of the Aceh fore-arc basin host a set of deeply-rooted, seaward-dipping backthrusts: main backthrust (MBT) and frontal backthrust (FBT), which we call north Sumatra backthrust system (NSBS). The FBT is imaged reaching the seafloor throughout the study area, whereas the MBT is imaged as a blind fault. Many landward-dipping imbricated thrusts (fore-arc high thrusts-FHT) are also observed below the fore-arc high, which along with the system of backthrusts have been responsible for uplifting the fore-arc high, shortening the Aceh Basin. On the landward slope of the fore-arc high, a strike-slip fault zone is imaged (termed West Andaman Fault - WAF - in accordance with previous studies), is readily interpreted as the product of the slip-partitioning at this oblique convergent margin, with a fraction of the arc-parallel slip localizing at the boundary between fore-arc high and fore-arc basin. Our results allow us to establish the evolutionary history of the thrust faults, strike-slip fault zone and the fore-arc basin. We suggest that the major structural features including backthrusts (MBT, FBT), fore-thrusts (FHTs) and the fore-arc high were developed during the Miocene, and that the growth of the fore-arc high accelerated in the Pliocene onwards owing to a sudden increase in sediment volume provided by the Nicobar fan.

1. Introduction

Most convergent margins have a conspicuous history of tectonic erosion and/or accretion (Moore and Silver, 1987) in which the growth of the fore-arc, i.e., the domain extending between the deformation front and the magmatic arc (Dickinson and Rich, 1972; Dickinson, 1995), is directly linked with accretionary wedge mechanics. Many numerical (Willett et al., 1993; Mannu et al., 2017) and experimental (Byrne et al., 1993; Larroque et al., 1995) studies have been carried out and marine geophysical field datasets have been acquired to understand the evolution fore-arc basins, for instance the San Blas Basin (Silver & Reed, 1988), Tobago Trough (Torrini et al., 1985; Westbrook et al., 1988; Torrini & Speed, 1989), Hikurangi fore-arc Basin (Lewis and Petinga, 1993), central Aleutian fore-arc Basin (Ryan and Scholl, 1989), Manglares Basin (Marcaillou & Collot, 2008), Kumano fore-arc basin (Martin et al., 2010) and eastern Sunda fore-arc Basin (Lüschen et al., 2011).

In this study, we focus on the Sumatra subduction system, which is the site of oblique convergence of the Indo-Australian plate beneath the Eurasian continental lithosphere at a varying rate ranging from 63 to 43 mm/yr (Gahalaut et al., 2006) from south Sumatra to Andaman-Nicobar, respectively (Fig. 1a). The obliquity increases towards northern Sumatra causing slip partitioning between arc-parallel direction, resulting in the development of the strike-slip Great Sumatra Fault (GSF) on mainland Sumatra, and arc-normal direction responsible for slip on the megathrust. Aside from the GSF, two other faults have been suggested to accommodate a fraction of the arc-parallel motion in the western Sumatra fore-arc: the West Andaman Fault (WAF) and the Mentawai Fault (MF). The nature of the WAF, which borders the southwestern margin of the Aceh fore-arc basin, has been highly debated as different types of faulting are observed in the area. This fault has been commonly interpreted as a right-lateral strike-slip fault system based on bathymetry data and the presence of positive flower structures on

* Corresponding author.
E-mail address: dghosal@iitk.ac.in (D. Ghosal).

https://doi.org/10.1016/j.jseaes.2021.104814
Received 30 March 2020; Received in revised form 2 February 2021; Accepted 4 April 2021
Available online 8 May 2021

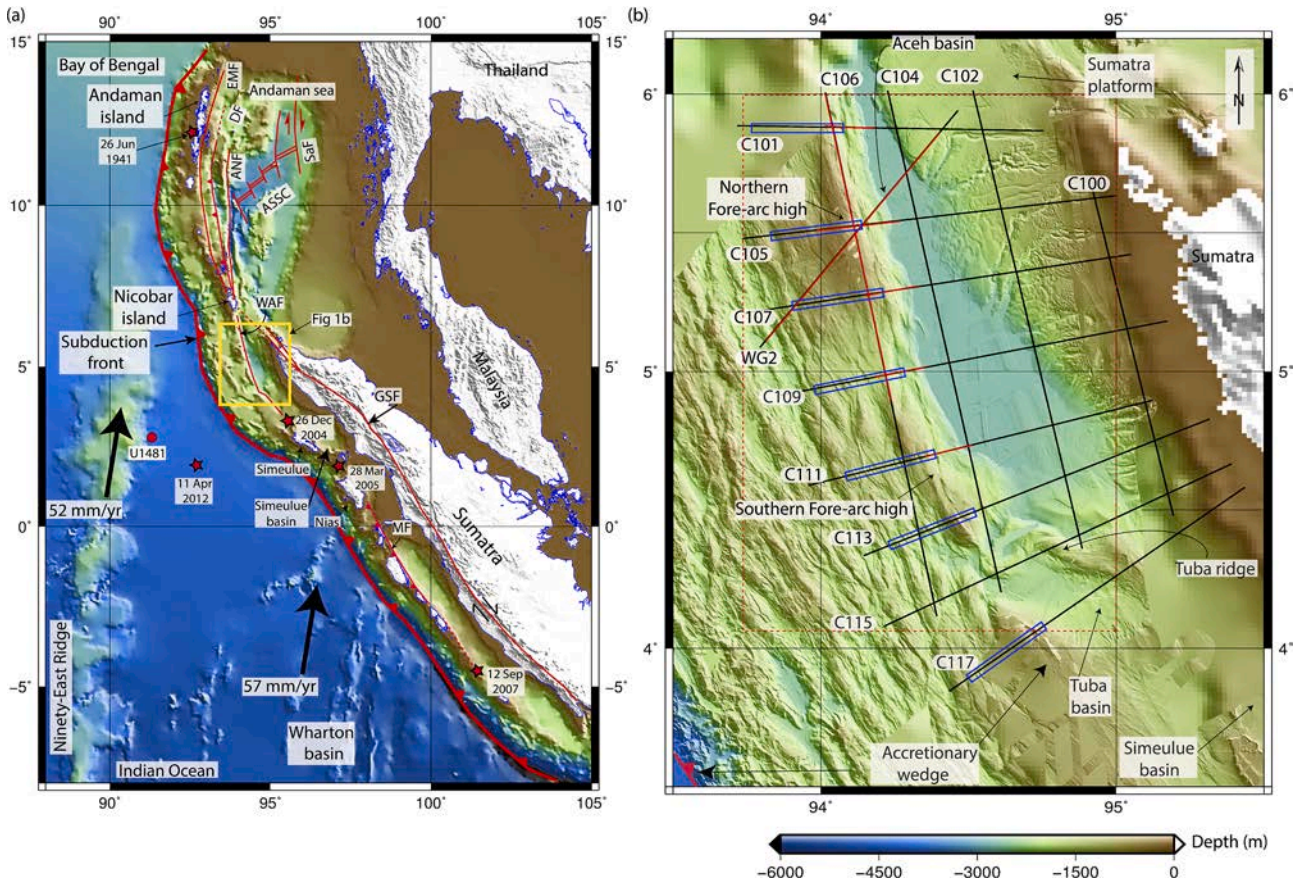

Fig. 1. (a) Tectonic map of Sumatra-Andaman subduction system. Major earthquakes are shown by red stars. Location of the hole U1481 from the expedition IODP 362 is marked by a red solid circle. EMF: Eastern Margin Fault, DF: Diligent Fault, ANF: Andaman-Nicobar Fault, WAF: West Andaman Fault, SaF: Sagaing Fault, GSF: Great Sumatra Fault, ASSC: Andaman Sea Spreading Center. Yellow rectangle marks the region shown in Fig. 1b. (b) Blow up of the study area. Bathymetry data were compiled from the French surveys (Singh et al., 2008) with GEBCO data set in the background. Seismic lines (WG2 and TGS) are marked by black lines. Seismic images shown in Fig. 4 and Figs. 5–8 are marked with blue boxes and red lines, respectively, and. Red dotted box indicates the region enclosed in Fig. 9.

shallow seismic data (Martin et al., 2014), possibly accommodating arc-parallel slip (Curray, 2005; Mosher et al., 2008; Berglar et al., 2010). Using deep seismic reflection and multibeam bathymetry datasets, Chauhan (2010) showed instead that the main tectonic structures consist of a set of backthrusts, originating at the subduction interface (Singh et al., 2012) at ~ 20 km depth, separating the accretionary wedge fore-arc sediments in the southwest from the continental block in the northeast, and emerging at the southwest boundary of the Aceh fore-arc

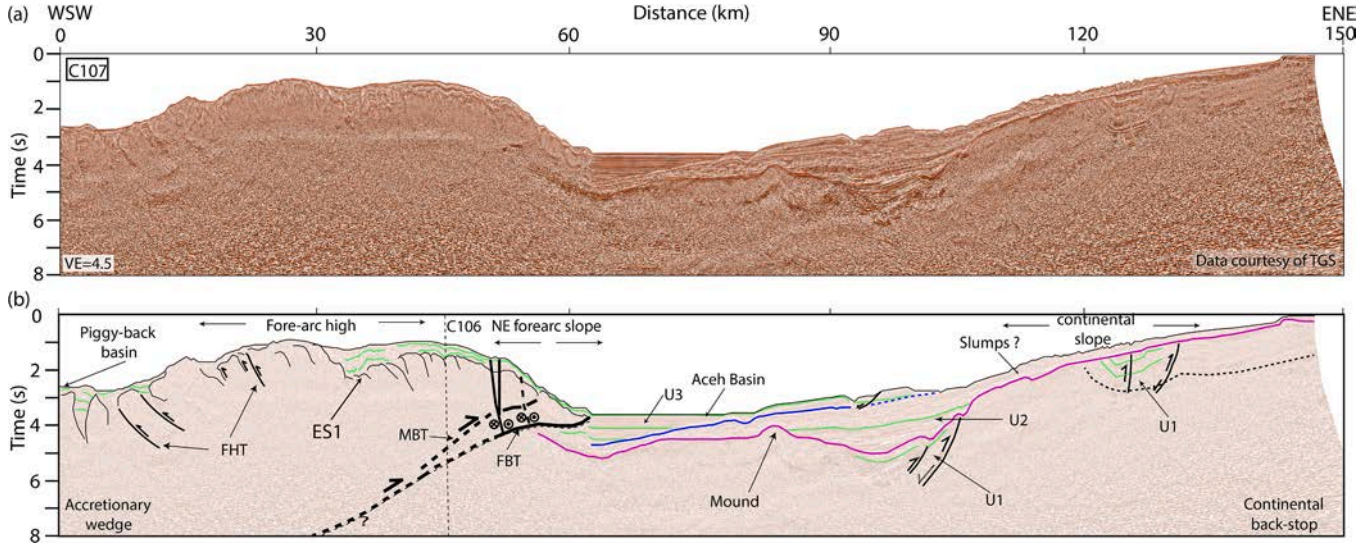

Fig. 2. Time migrated seismic image of C107 (TGS); (a) uninterpreted and (b) interpreted. FHT: Fore-arc high thrust; MBT: Main backthrust, FBT: Frontal backthrust. Different sedimentary units (U1, U2, U3) are marked in green; basal unconformity (purple), ES2 (blue), faults (black).

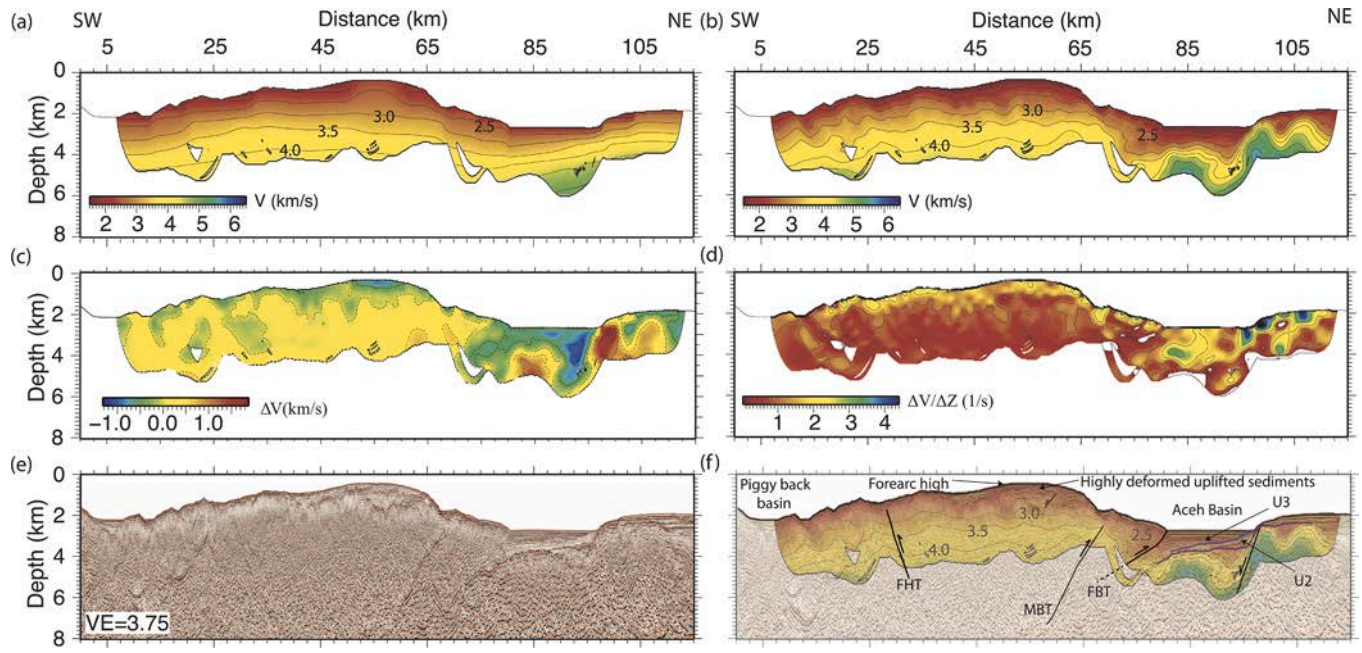

Fig. 3. (a-d) Travel time tomography inversion results; (a) Starting model (b) Best-fit model (c) Difference between starting and best-fit model (d) Vertical velocity gradient (e) Uninterpreted prestack depth migrated section (f) Superimposition of interpreted prestack depth migrated section and best-fit model. MBT: Main backthrust, FBT: Frontal backthrust, FHT: fore-arc high thrust. U3: unit 3 deposits.

basin.

The Mentawai Fault Zone in the central and southern Sumatra was initially interpreted as a flexural bulge or backthrust (Karig et al., 1979), then as a strike-slip fault (Diament et al., 1992). Positive flower structures, typical of strike-slip or transpressional systems, have been observed in seismic reflection profiles offshore southern Sumatra (Schlüter et al., 2002). It was suggested that the MF and the WAF connect offshore Sumatra near Nias Island (Malod and Kamal, 1996; Mosher et al., 2008). Using industry high-resolution multichannel seismic data, Mukti et al. (2012) concluded that the MF is a backthrust, which is consistent with the presence of relocated thrust earthquakes observed along the seaward margin of the Sumatra fore-arc basin between Nias Island and Sunda Strait.

Here, we aim to characterize the nature of the complex fault system located at the boundary between the fore-arc high of the north Sumatra accretionary wedge and the Aceh fore-arc basin and to provide an evolutionary model of the Aceh fore-arc basin. We use a grid of eleven unpublished industry multi-channel seismic reflection profiles covering the whole of the Aceh Basin and adjacent fore-arc high, a portion of a long-offset multi-channel seismic profile already presented in a different processed form by Chauhan et al. (2009) and Singh et al. (2012), and multibeam swath bathymetry data compiled from a variety of marine surveys.

2. Study area

The study area, located offshore NW Sumatra, contains a broad accretionary wedge, a distinct fore-arc high, and a wide fore-arc basin (Aceh Basin) (Figs. 1 and 2). The triangular-shaped, ~ 260 km long Aceh Basin, is bordered in the east by the Sumatra platform and in the west by the fore-arc high of the inner accretionary wedge. It extends between Nicobar Island in the north and Tuba ridge in the south, which separates it from the Simeulue Basin. The Aceh Basin, with a maximum water depth of 2500 m and consisting of thick well-stratified sedimentary deposits, has developed on top of a high-velocity crystalline backstop at depth (Singh et al., 2012) (Fig. 1b). West of the Aceh Basin, the landward slope of the fore-arc high has been identified as hosting a strike-slip fault, the West Andaman fault (WAF). The WAF has been suggested to originate adjacent to the Andaman Islands, proceeding southwards west of the Aceh Basin and merging with the Mentawai Fault (MF) in the south (Diament et al., 1992; Berglar et al., 2010). The Great Sumatra Fault (GSF) lies farther arcward; its submarine portion, offshore the northern tip of Sumatra, was the subject of a previous study (Ghosal et al., 2012). North of our study area (Fig. 1a) three more faults accommodate strike-slip and compressional deformation: the Andaman-Nicobar Fault (ANF), Eastern Margin Fault (EMF), and the Diligent Fault (DF) (Singh et al., 2013). The ANF is primarily strike-slip in nature and connects the GSF on the Sumatra mainland to the Sagaing fault (SaF) in Myanmar, passing through a series of spreading centers in the Andaman Sea (Fig. 1a) (Curray 2005; Singh et al., 2013; Singh and Moeremans, 2017). The EMF and DF are reported as normal and thrust faults (Singh and Moeremans, 2017; Moeremans and Singh, 2014), respectively, and extend northward through the Andaman region. The oceanic plate seaward of the study area carries the 6000 km long, 120 km wide and 15 km thick Ninety-East Ridge (NER) (Grevemeyer et al., 2001), which impinges on the deformation front of the Andaman-Nicobar segment at 8° N (Singh and Moeremans, 2017), as well as a series of N-S trending reactivated fracture zones.

3. Data and methodology

In this study we use high-resolution bathymetry data, one deep seismic reflection profile (WG2) and eleven industry-standard high-resolution seismic profiles.

3.1. WG2 data

During July-August 2006, coincident deep seismic refraction and reflection profiles were shot using the French R/V Marion Dufresne and the WesternGeco M/V Geco Searcher vessels carrying 8,260 cubic inch and 10,170 cubic inch airgun array sources, respectively. The WG2 profile (Fig. 3) was oriented 20° anticlockwise from a direction orthogonal to the trench (Fig. 1b). It was instrumented with 56 ocean-bottom seismometers (OBS) spaced at 8.1 km, and shots were fired at 150 m intervals (Chauhan et al., 2009). A 12 km long Q-marine streamer was deployed at 15 m water depth to record deep seismic reflection

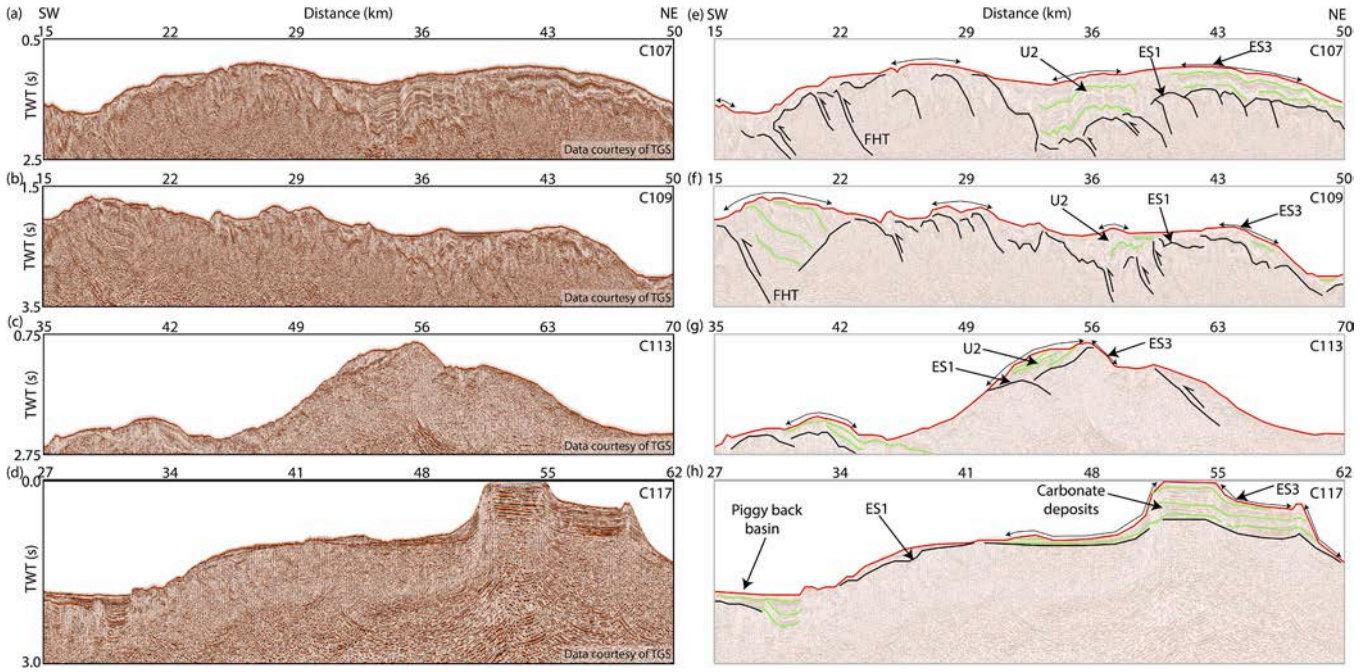

Fig. 4. Seismic images of the fore-arc high: (a-d) uninterpreted and (e-h) interpreted. Green: sedimentary deposits, black: compact accretionary wedge. ES1: erosional surface; Erosional surface ES3 is marked by double headed arrow; FHT: Fore-arc high thrust.

energy at 50 m shot interval (Singh et al., 2012). The streamer contained 3,832 individual hydrophones spaced at 3.125 m, with individual hydrophone signals later grouped at 12.5 m after application of a digital filter (Martin et al., 2000). The WG2 profile covers the trench deposits, accretionary wedge, fore-arc basin, Sumatra platform, and arc-related basins. The detailed architecture of the trench deposits and that of arc-related basins have been previously investigated by Ghosal et al. (2014, 2012, 2009). This study focuses on the 125 km long segment that covers the part of the accretionary wedge and fore-arc basin (Fig. 1b and Fig. 2).

The refracted phases in the 12 km streamer data are crucial to obtain a high resolution velocity-depth model of the subsurface. We downward continue (Ghosal et al., 2012, 2014) all the shot gathers from the streamer data to the seafloor to bring the refracted arrivals at the near offset as first arrivals. Downward-continued gathers are then picked using a semi-automatic technique and first arrival picks are used as input for the travel time tomography method (Van Avendonk et al., 2004). A 2D velocity-depth model, adapted from the coincident OBS tomography results (Chauhan et al., 2009), is used as a starting model (Fig. 3a) in which the grid interval is kept as 50 m. In forward modelling, the synthetic travel times are computed using the shortest path method (Moser, 1991) and the ray coverage is computed by the Derivative Weight Sum (DWS) (Scales, 1987). We use the least squares method to carry out the inverse modelling, in which the misfit between the observed and synthetic travel time is minimized iteratively, leading to the best-fit model (Fig. 3b). The model smoothness/roughness are controlled by tuning the roughness matrix, which contains both first and second-order spatial derivative matrices, whereas the model artifacts during inversion are suppressed by a proper choice of the damping constant (Van Avendonk et al., 2004). Further details of the methodology and parameter estimation for the travel time tomography are described in S1.

Fig. 3c shows the difference between the starting velocity model and the best-fit model (here we present only the part of the model which is sampled by the rays - the rest is masked). The depth extent of ray coverage is high (3–4 km below seafloor) below the fore-arc high and reduces to 2 km below the NE fore-arc slope, and again increases to 3–4 km below the Aceh Basin. It is lowest farther east below the continental slope. This is reasonable since the bathymetry along the WG2 profile varies significantly from the fore-arc high to Aceh Basin, the nature of the ray paths varies laterally. Small wavelength structures are recovered by our tomographic inversion below the fore-arc high, Aceh Basin and continental slope (Fig. 3b-d). The tomographic velocity-depth model is further used for prestack depth migration (Fig. 3e) and the final depth-migrated image is used for interpretation (Fig. 3f). The details of the pre-stack depth migration are provided in the supporting material.

3.2. Industry seismic reflection data

In 2010, a total of 11 high-resolution multi-channel seismic (MCS) lines were acquired by TGS Nopec across (C101, C105, C107, C109, C111, C113, C115, C117) and along (C100, C102, C104, C106) the strike of the Aceh fore-arc basin, with a line spacing of 20 km (Fig. 1b). A 7.95 km long streamer towed at 7 m water depth and a 3,940 cubic inch source towed at 5 m water depth, with a shot interval of 37.5 m, were used for the acquisition. The dip profiles traverse the fore-arc high, fore-arc slope, Aceh Basin and shelf deposits. In this study we only show selected portions of the seismic profiles which are used to discuss the features of interest in this study (the fault system, fore-arc high, fore-arc slope and Aceh Basin). Although the recorded data were 12 s long, we have used only the first 8 s TWT and their blow ups to describe the salient structural features. The datasets are resampled to 4 ms and time migrated using a Kirchhoff pre-stack migration technique (Fowler, 1997).

4. Results

4.1. Aceh Basin and continental slope

The triangular-shaped Aceh Basin is ~ 10 km wide in the north near Nicobar Island and becomes ~ 50 km wide near the Tuba ridge in the south (Fig. 1b). The basin is filled with different sedimentary units ranging in thickness from ~ 1–1.5 s TWT in the north to ~ 4 s TWT in the south near the Tuba ridge. Three major units can be distinguished: the top most parallel laminated deposits (unit 3 - U3), the semi-transparent to transparent, sub-parallel westward dipping and deformed sedimentary unit (unit 2 - U2) and the bottommost sediments (unit 1 - U1), which

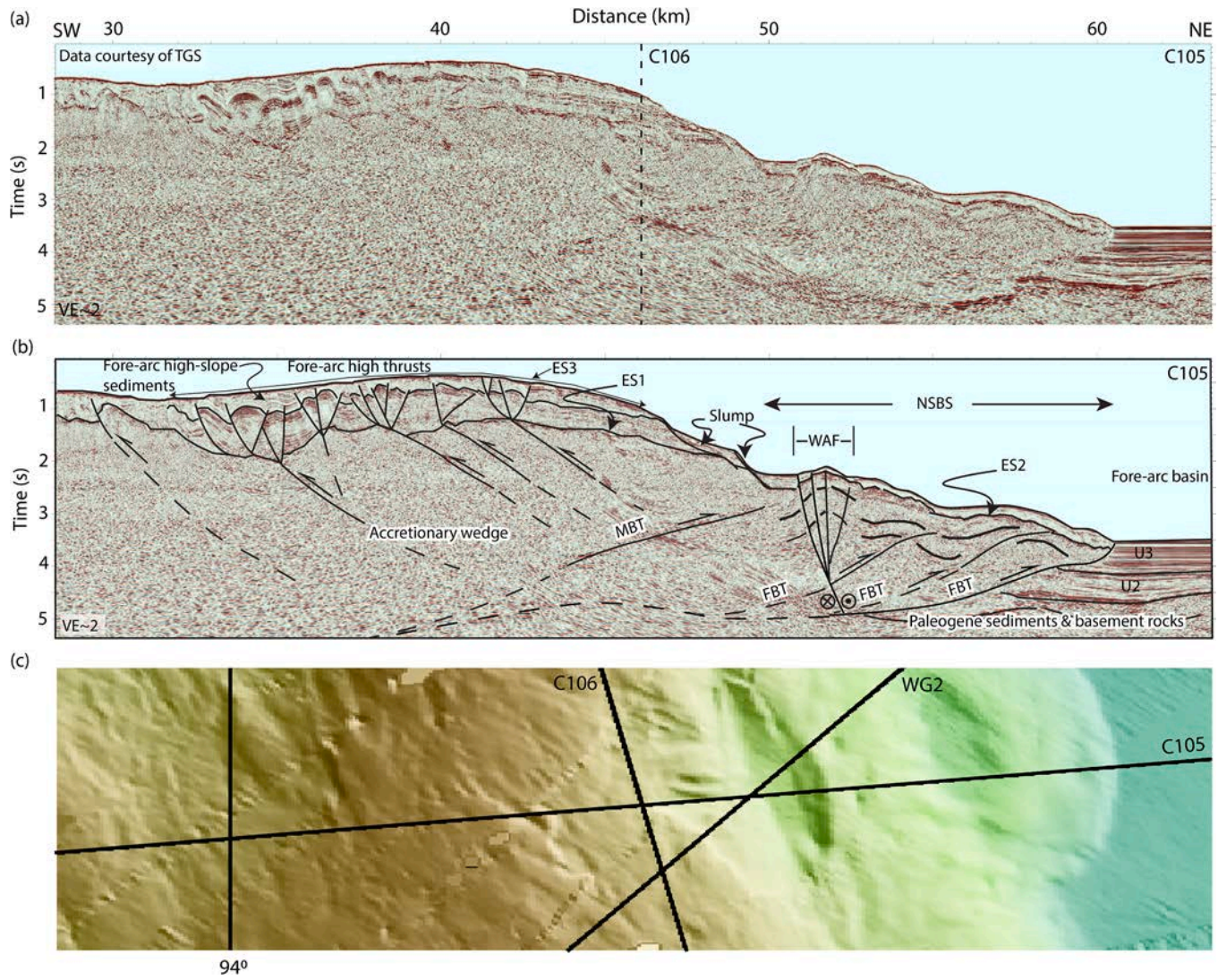

Fig. 5. Time migrated sections of C105: (a) uninterpreted and (b) interpreted. MBT: Main backthrust, FBT: Frontal backthrust, PFBT: paleo FBT, RFBT: Recent FBT; WAF: West Andaman Fault. Different deposits (U2, U3) are marked. Cross-over with profile C106 is marked by a dashed line. WAF cross-cuts the MBT and FBT and forms push-up structure. Erosional surfaces (ES1, ES2 and ES3) are marked; (c) C106, C105 and WG2 locations are shown on the bathymetry.

are also deformed with a distinctly higher reflection strength. U1 is underlain by older basement rocks (Fig. 2). The velocity of U3 and U2 deposits ranges from 2 to 3 km/s whereas U1 deposits contain high velocity materials (~3.5–4 km/s) (Fig. 3). A sudden increase (~5.5 km/s) in velocity occurs below the Aceh Basin, confirming the crystalline origin of basement rock, flooring the Aceh Basin (Fig. 3). U3 onlaps U2 below the continental slope, which contains several mass transport deposits indicating gravity slumping or earthquake induced landslide deposits (Fig. 2). U1-U2 and U2-U3 are separated by an irregular, basal erosional unconformity (purple in Fig. 2) and an angular unconformity (blue in Fig. 2), respectively. The basal unconformity is irregular in shape and a mound is present in it. The eastern flank of the Aceh Basin at depth show subsidence-associated normal faulting (Fig. 3f), but the folding in the U1 suggests compression and possibly reverse faulting and re-activation of normal faults. The western flank of the basin is bounded by the frontal backthrust (FBT).

4.2. Fore-arc high, Fore-arc high sedimentation and Fore-arc high thrusts (FHT)

The fore-arc high is well developed in most of the across-strike profiles acquired in the northern part of the basin (Fig. 1b). At the western (seaward) end of profile C107 (Fig. 2), the fore-arc high starts with a thinly sedimented basin, intersected by a small ridge-like structure, followed farther east by highly folded and faulted shallow sedimentary deposits with a thickness ranging between 1 and 1.5 s TWT (Figs. 2–5). The reflectivity of these fore-arc sedimentary deposits resembles the reflectivity of the U2 observed (Fig. 5) in the Aceh Basin. The local erosional surface is marked by ES3. The degree of erosion increases southeastward as is evident from the profile C113 (Fig. 4c and 4 g) where the U2 deposits are almost eroded and tilted south-westward. The tilt angle of these deposits confirms that they have undergone a severe uplift either before erosion initiated or during the erosion process. In profile C117, the fore-arc high is overlain by horizontal layers, which may be carbonate deposits as observed in Aubert and Droxier (1996); on this profile the U2 deposits are completely eroded. The velocity-depth model (Fig. 3b) shows the presence of a low-velocity (~2.5 km/s) region associated with U2 deposits (Fig. 3b and f) at a very shallow depth (~100–200 m depth below seafloor), which further indicates that these deposits are less compacted. Although the reflectivity below the seafloor in the fore-arc high is very poor, a number of landward-dipping, imbricated fore-arc high thrusts (FHT) are clearly observed in the accretionary wedge down to a depth ranging between 1.5 and 3.5 s TWT (Fig. 4). A NE-dipping velocity low (Fig. 3c) is

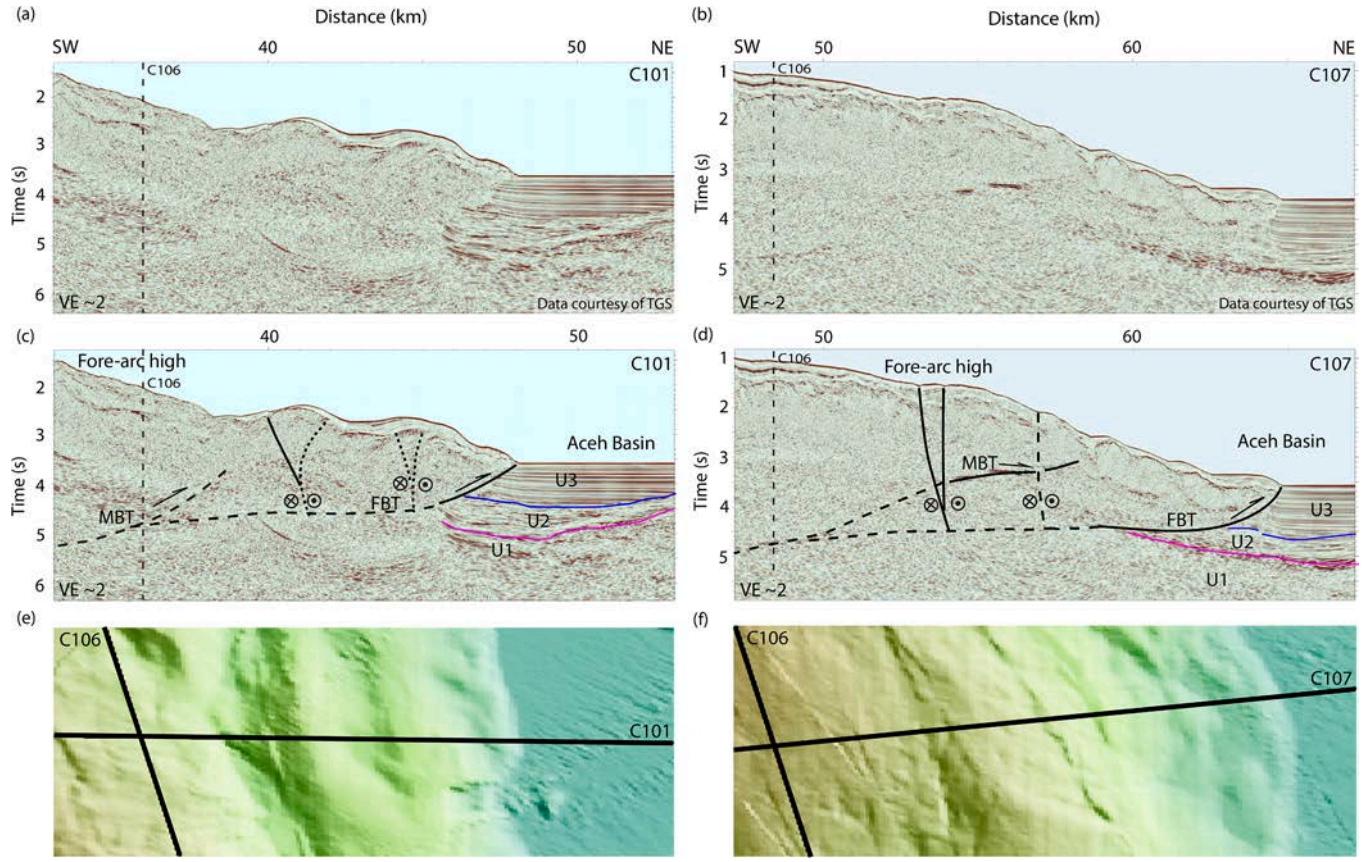

Fig. 6. Time migrated sections of profiles C101 and C107: (a, b) uninterpreted and (c, d) interpreted. Cross-over with profile C106 is marked by a dashed line; (e) locations of C106 and C101 and (f) C106 and C107 are shown on the bathymetry.

observed at 25 km distance from west along the FHTs, indicating these faults acted as pathways to the fluids coming from the deep accretionary wedge under the effect of compression. At the Sumatra subduction zone, the presence of fluids along the accretionary wedge backthrust has been reported in the Mentawai region (Singh et al., 2011a), but the possible presence of fluids along imbricated thrusts would be a new observation. The base of the unit U2 is marked by an erosional surface ES1 (Fig. 5). The fore-arc high is well developed between profiles C101 and C107 in the north, followed by the absence of a high south of profile C107 in the area of profile C109 (area that we refer to as a "depression" later on); then in the south, between profiles C109 and C115 (Fig. 1b), the high is present again (but less prominent than in the north). We call these highs northern and southern fore-arc high, respectively (Fig. 9).

4.3. North-eastern Fore-arc slope and associated fault systems

The landward slope of the fore-arc high connects the fore-arc high with the Aceh Basin. Two major fault systems are encountered in this area: backthrusts and strike-slip faults. We distinguish two types of backthrusts: frontal backthrust (FBT) and main backthrust (MBT), which together form the north Sumatra back-thrust system (NSBS). The salient features of each of these faults are described in the following sections.

4.3.1. Main backthrust (MBT)

The main backthrust (MBT) is a seaward dipping thrust, observed from ~ 6 s TWT beneath the fore-arc high up to the near-seafloor (Figs. 2, 3 and 5). The MBT is well imaged below the northern (Figs. 5 and 6) and southern fore-arc highs (Fig. 7). From the across-strike profiles - C105 and C107 (Figs. 5 and 6), one can notice that the MBT does not reach the surface, i.e. it is a blind thrust; in some places it lies beneath a small basin. Because the MBT does not reach the surface, it is possibly inactive. The high velocity (~3–4 km/s) (Fig. 3b and c) sediments lying on the hanging wall side of the MBT from 25 to 45 km distance at ~ 4 km depth suggest these deposits are highly compacted (similarly to what was observed by Huot and Singh, (2018) in the Mentawai region). Moreover, we notice an uplift of the fore-arc high by ~ 3.0 km with respect to the base of the Aceh Basin (Fig. 3b). The strike-parallel profile C106 (Fig. 1b and Fig. 8) shows a reflection extending over a distance of ~ 120 km, which is not a seafloor multiple and matches the top of MBTs observed in the across strike profiles, indicating that this reflection is the MBT. From the northern fore-arc high to the central depression, the shape of the MBT reflector in two-way travel time mimics the bathymetry. The reflection along this fault shows negative polarity with respect to the seafloor, suggesting that it could be due to the presence of fluid along the MBT. At some locations, for instance at ~ 120–130 km distance from the SE (Fig. 8), the MBT consists of two reflections, which might correspond to the top and bottom of a damaged zone associated with this fault. The deepening of the MBT towards SE is clearly observed (Fig. 1b). Thus, the absence of MBT farther SE (between 75 and 90 km distance) could be due to limited penetration of the seismic energy at a greater depth.

4.3.2. Frontal backthrust (FBT)

The seaward-dipping frontal backthrusts (FBTs) separate the landward slope of the fore-arc high from the Aceh Basin. The sedimentary deposits observed below the fore-arc slope and in the unit U2 (Fig. 5) at ~ 55–59 km distance and at 4–4.5 s TWT at the SW edge of the Aceh Basin are folded and deformed by a sequence of FBTs - paleo FBT (PFBT) and recent FBT (RFBT); the FBTs are younger than those deposits (Figs. 5, 6). The top of the sedimentary deposits is marked by an erosional surface (ES2), which separates the overlying recent U3 deposits from the underlying deformed sedimentary units. Fig. 3c shows a

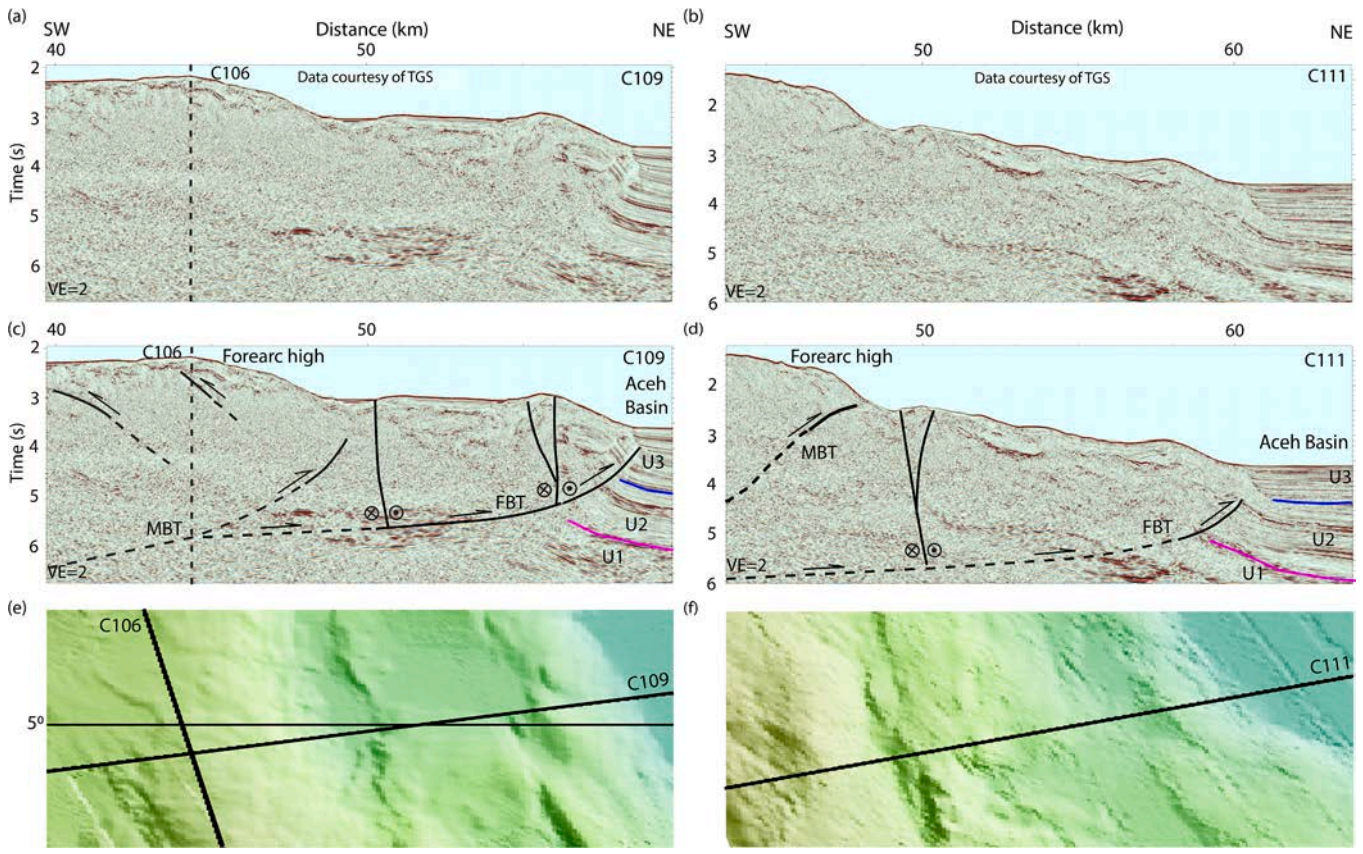

Fig. 7. Time migrated sections of profiles C109 and C111: (a, b) uninterpreted and (c, d) interpreted. Cross-over with profile C106 is marked by a dashed line, (e) locations of C106 and C109 and (f) C106 and C111 are shown on the bathymetry.

velocity low along the FBTs indicating either a lower degree of compaction associated with the hanging wall deposits or the fact that these deposits might be saturated with fluid. In the northern part of the Aceh Basin, the recent FBT reaches the seafloor indicating that it is active (Figs. 5 and 6), whereas in the south (Fig. 7) it does not come to the seafloor, but it deforms the unit U3 syntectonically which is evident from the thinning of this unit at ~ 60–61 km distance and at ~ 3.5–4 s TWT (Fig. 7b, d and f) at the SW end of the Aceh Basin. This indicates that the FBT is active throughout the northern and southern fore-arc. We can also notice that the distance between the MBT and FBT increases southward (Fig. 9) and the separation reaches its maximum at the southern end of the Aceh Basin (Fig. 9).

4.3.3. *Strike-slip faults*

A set of shallow strike-slip faults is also identified on the landward slope of the fore-arc high as a sharp, mostly linear fault trace in the bathymetry with the presence of right-stepping en echelon scarps (bounding graben-type structures) in the bathymetry (Fig. 1b and Fig. 9), and showing the presence of positive flower structures on the seismic profiles (Figs. 5 and 7). The “en echelon” faulting is well developed in the depression between northern and southern fore-arc highs (Fig. 9). We refer to this strike-slip fault as WAF in accordance with earlier studies (e.g. Berglar et al., 2010; Martin et al., 2014). The WAF cross-cuts the preexisting FBTs and ES2 (Fig. 5), and are originating from the top of the FBT plane, inferring that the strike-slip faults are younger than the FBTs and ES2, and accommodate transpressional deformation. From the bathymetry (Fig. 1b and Fig. 9 it is clear that the strike-slip WAF runs very close to the MBT except in the depression region where the MBT displays a step and the WAF displays two branches-WAF1 and WAF2 (Fig. 9b).

5. Discussion

5.1. *Age estimation of different tectonic units*

Due to the lack of drilling results in the basin, we have estimated the age of the sedimentary units from existing literature (Beaudry and Moore, 1985; Izart et al., 1994; Berglar et al., 2010; Samuel et al., 1997) and found that the U3 is of Pliocene to Recent deposits whereas U2 is of the Mid-Late Miocene and the bottommost U1 is of Pre-Neogene. Using drilling datasets from the Simeulue Basin, Berglar et al. (2010) documented that the age of the basal unconformity (between U1 and U2) below the Aceh Basin is of base Neogene age. Therefore, the age of the unit U1 in the basin must be older than that of the basal unconformity. We identified three sets of erosional surfaces (ES1, ES2 and ES3) in the accretionary wedge in Figs. 5 and 6 in which the erosion surface ES1 in the wedge (Figs. 5, and 10) and the basal unconformity in the Aceh Basin are marked as the truncated top of U1 (Figs. 5-6 and 10). The irregular shape of the basal unconformity and the presence of a mound (Fig. 2) on it suggest that the basement experienced severe lateral compression during the subduction process and had undergone erosion in the course of time. It is difficult to comment whether these two erosional events started simultaneously or not, but it is certain that they exist and the deposition stopped for a very long time making the top surface of the accretionary wedge exposed and eventually eroded. The top surface of U2 marked as another erosional surface (ES2) must be younger than that of ES1 but older than that of the ES3.

5.2. *Evolution of the fore-arc high and associated fault systems*

Deposited sequences and main tectonic features observed in the fore-arc basin constrain the tectonic evolution of the study area. A simplified

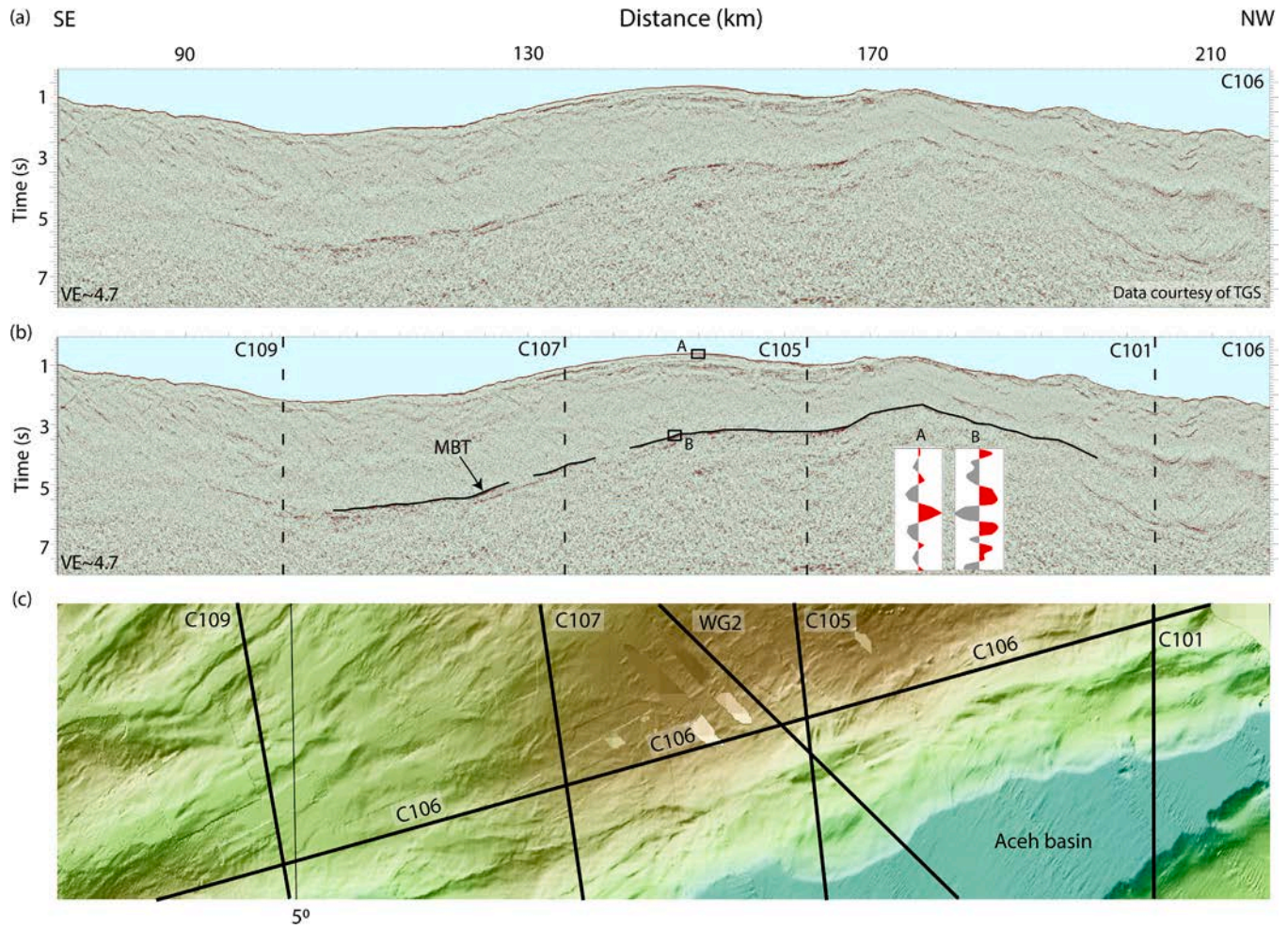

Fig. 8. Time migrated section of along-strike profile C106: (a) uninterpreted and (b) interpreted. Line crossings with profiles C101, C105, C107, and C109 are marked by dashed lines. MBT (B) shows reverse polarity with respect to the seafloor (A), (c) locations of C106, C101, C105, WG2, C107 and C109 are shown on the bathymetry.

sequence of major tectonic events is described in Fig. 10.

5.2.1. Initiation of Aceh Basin formation

In the pre-Neogene period there was local subsidence associated with the Aceh Basin region producing the accommodation space for sediment deposition (Fig. 10a). The OBS tomography results and gravity datasets (Singh et al., 2012) indicated the possible presence of crystalline basement, which is further confirmed by results from high resolution multichannel seismic tomography of downward continued streamer data (Fig. 3b). Based on field datasets, Samuel et al. (1997) reported that extension affecting basement materials and initiation of basin formation in Nias and adjacent areas took place in mid-Oligocene time. One can argue that the episode of basement extension in our study area could be contemporaneous to that on and near Nias. Normal faulting of the acoustic basement along the NE flank of the Aceh Basin suggests basin subsidence (Fig. 3). The basin was supported in the east by the backstop and in the west by the accretionary wedge of that time (Fig. 10a). Seismic velocities of ~ 6 km/s suggest the backstop of continental origin that has also been inferred in Central and Southern Sumatra (Kopp et al., 2001; Kopp and Kukowski, 2003; Mukti, 2013).

The unit U1 then accumulated on the basin floor in pre-Neogene time by terrigenous materials resulting from the erosion of the continents and the accretionary wedge. The erosional (basal) unconformity marked in purple color in Figs. 2 and 10 indicates that top of U1 was exposed for a very long time and underwent erosion. In pre-Neogene, the fore-arc high was not as topographically elevated as it is at present.

5.2.2. Development of accretionary wedge, MBT and FHT

Evidence of highly folded and faulted sedimentary deposits, presence of high-velocity sedimentary deposits (Fig. 3) with lack of stratified sedimentary structures in the fore-arc (Figs. 2, 4 and 5) indicate that these deposits must be very old and underwent severe stages of deformation and thus suggestive of lateral compression associated with the subduction process (Fisher et al., 2007). It is difficult to comment when exactly the MBT started to develop. Hall (2012) estimated that the subduction process in Sumatra started from middle Eocene time. Mukti (2013) reported an age of the Bengkulu fault zone of middle Eocene, whereas the backthrusts developed in early to middle Miocene time in the Mentawai region (Mukti et al. 2012). Backthrusting is also observed in the Andaman region and Singh and Moeremans (2017) reported that the development of backthrusts also took place in early Miocene time. Samuel et al. (1997) reported an uplift phase in Nias in early Miocene. As our study area lies between the aforesaid regions, the MBT in our study area might have also started developing in early Miocene time. Another important development in this time is the initiation of the frontal high thrusts (FHTs), which are imbricated thrusts and conjugate to the MBT. These two thrusts acted like two reverse kink bands (Mukti et al., 2012) of sandbox models (Davis et al., 1983; McClay et al., 2004).

After the development of MBT and FHT, the early to middle Miocene period was crucial for the development of the accretionary wedge in the study area. Many important tectonic events took place during this period. Core data recovered from the IODP expedition 362 (McNeill et al., 2017) reported that the Paleocene to middle Miocene period

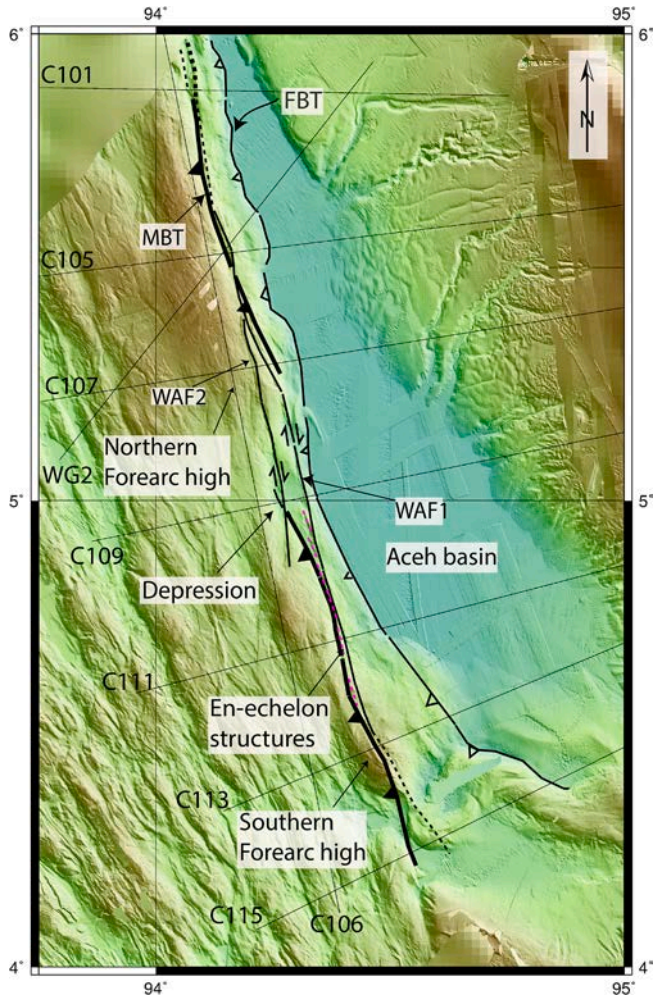

Fig. 9. Interpreted bathymetry map. WAF1 and WAF2: West Andaman fault (WAF) branches, red dashed lines: en echelon structures. FBT: frontal backthrust (thin black line with open triangles), MBT: main backthrust (thick black line with solid triangles).

experienced many hiatuses which caused several phases of erosions in the accretionary wedge, Aceh Basin deposits and the exposed basement rock during this period. From Late Miocene onwards, the FHTs actively took part in the development of the fore-arc structure and uplift of the unit U2 which eventually deformed and tilted. The similarity in the reflectivity of U2 deposits in Aceh basin and the sediments on the fore-arc high (Fig. 5) indicate that U2 formed in a fore-arc basin environment, but have since been folded, faulted and uplifted. An increase in the degree of contraction rotated the FHTs landward and deformed the U2 sediments that reside on top of the fore-arc high.

5.2.3. Development of FBT

The deformation of U2 sediments and the growth of the accretionary wedge continued during late Miocene-Pliocene period. Evidence of folded and deformed sedimentary sequences along with FBTs below fore-arc slope and in the U2 deposits (Fig. 5) indicate that the formation of the FBT initiated a landward migration of the accretionary wedge during late Miocene reducing the accommodation space in the Aceh basin (Fig. 10). This further infers that the original Aceh fore-arc basin was located in the area of the current fore-arc high, and moved farther NE due to landward migration of FBT. The top of the deposits in the fore-arc high has also been eroded (Figs. 4 and 5), which could have been caused by either a tectonic uplift of the high or a sea-level fall. The combined effect of slip on the MBT, FHT and newly formed FBTs contributed to further uplift of the fore-arc high. Lee and Lawver (1995) reported that the obliquity of plate convergence decreases by ~ 18° during lower to upper Miocene time which again eventually increased the trench normal component of slip increasing intensity of the backthrusting in this region. Syntectonic development of U3 over the fore-arc high and Aceh Basin onlaping the north-eastern continental slope deposits indicates that the development of the FBT and deposition of U3 were contemporaneous (Figs. 7, 10).

5.2.4. Landward migration of FBT and development of WAF

As motion on the FBT continued, the wedge and fore-arc high started to grow more landward reducing the accommodation space of the Aceh Basin. During Pliocene to Recent times, the obliquity of the plate convergence increased (Lee and Lawver, 1995) and thus a part of the slip along the FBT might have partitioned along the arc-parallel direction forming the strike-slip fault on the fore-arc, which we refer to here - similarly to earlier studies - as West Andaman Fault (WAF). As Singh et al., (2012) showed a seismic image of the FBT/MBT system below the fore-arc high down to ~ 20 km depth, we suggest that slip partitioning occurs above the FBT. The development of the WAF was influenced by the development of the GSF on mainland Sumatra and that of the ANF farther north (Fig. 1b), both of which are dextral strike-slip faults. The age of WAF is uncertain. Curray (2005) reported that WAF could be older than Pliocene but he did not have any evidence to support that. Berglar et al., (2010) reported that the strike-slip faulting in the Simuelue basin was initiated in late Miocene and affected the upper sedimentary sequences in the Aceh basin. WAF in our study area crosscuts the PFBTs and thus one can speculate that the development of the WAF took place in late Pliocene onwards as the strike-slip system in the Sumatran region is very young and initiated ~ 2 Ma onwards (Hall, 2012, Sieh and Natawidjaja, 2000). As the uplift continued in Pliocene onwards and a rapid uplift is recorded in Nias area (Samuel et al., 1997) in the latest Pliocene-Pleistocene time, the fore-arc high either reached sea level or exposed to the surface causing erosion of U3 (ES2) and a part of U2 from the top of the accretionary wedge, forming the erosional surface marked as ES3 (Figs. 5 and 10). The effect of this uplift is observed throughout the fore-arc in our study area but is more severe in the southern part of the fore-arc, where U2 is mostly eroded and only a remnant of U2 is visible in profile C113 (Fig. 4). The effect of the uplift is evident from the westward tilting of U2 on profile C113.

5.2.5. Contribution of Nicobar fan on backthrusting

Analyzing sediment core datasets from the IODP expedition 362, McNeill et al., (2017) reported that the sedimentation rate on the subducting oceanic plate offshore northern Sumatra was very high, ~250–300 m/Ma in the late Miocene-Pliocene (9.5–2 Ma) interval, which was suggested to be linked to the interplay of tectonic and climatic processes associated with the Himalayan mountain range. The oldest sediment deposited in Bengal fan, eroded from the Himalaya, is dated back to Oligocene (~23–28 Ma). Silts of early Miocene age, originated from the Himalaya, are observed in Bengal and Nicobar fan deposits. Both the Bengal and Nicobar fans started to grow prior to late Miocene, but the sedimentation rate started to increase from late Miocene (9–9.5 Ma) onwards in the Nicobar fan (McNeill et al., 2017). However, the fan deposits switched the route between Bengal fan and Nicobar fan, across the NER, during mid-Miocene to Recent times. The increase in sediment supply took place due to the inversion of the Bengal Basin related to tectonic shortening and exhumation of the Shilong Plateau (Bilham and England, 2001); and the main phase of surface uplift took place in late Pliocene (<3.5 Ma) increasing the sediment supply significantly (Najman et al., 2016). Moreover, the southern monsoon was also severe during mid-late Miocene, increasing the rate of erosion of the uplifted eastern plateaus. Since the sediment supply was very high in the Nicobar fan during the late Miocene-early Quaternary (9.5–2 Ma) period, it led to the development of a wide accretionary wedge offshore northern Sumatra. This very large supply of sediments

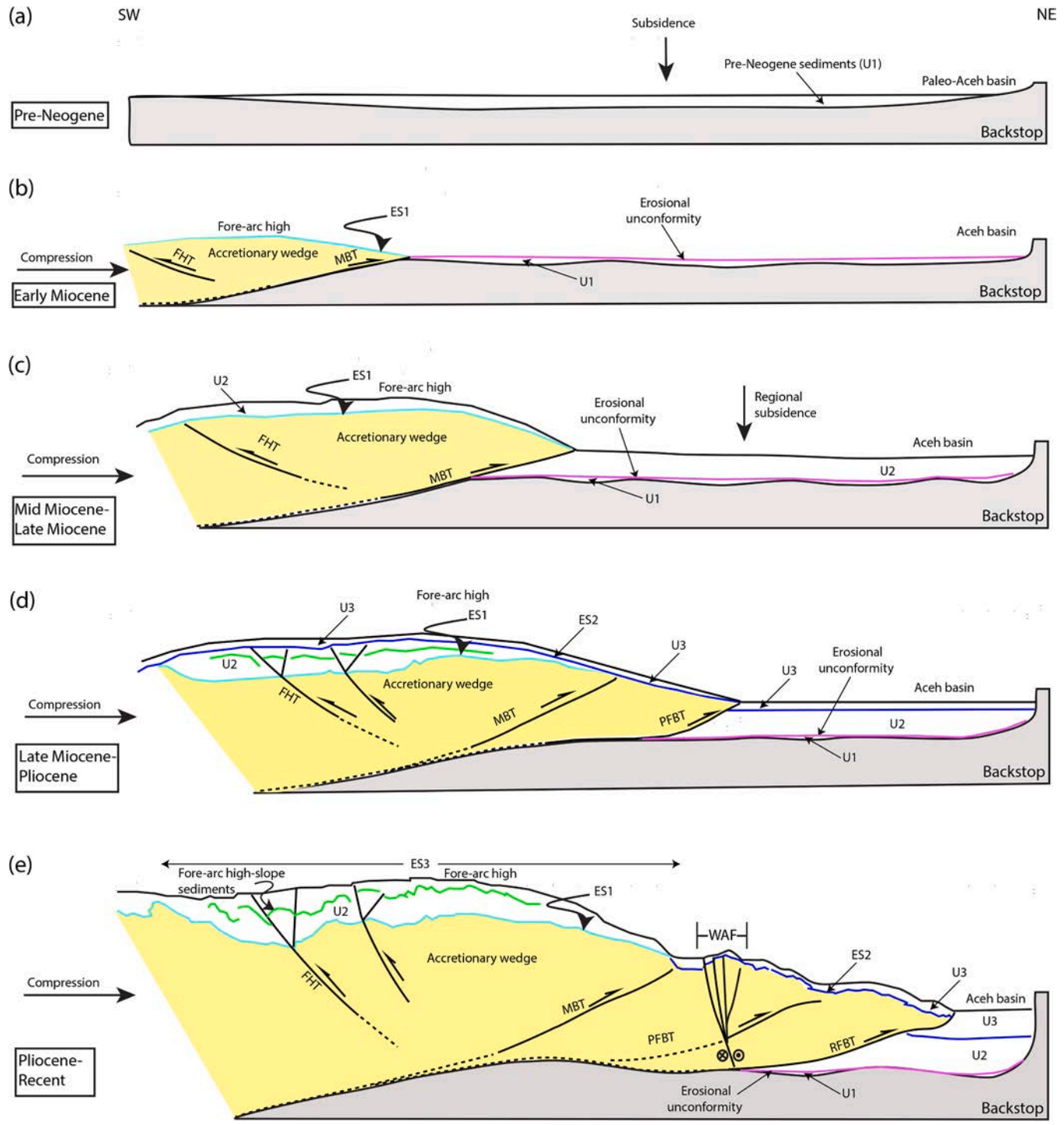

Fig. 10. Schematic diagram illustrating the fore-arc evolution. (a) Pliocene-Recent: Unit 3 deposited, WAF: West Andaman Fault, RFBT: recent FBT, PFBT: paleo-FBT, ES3: erosional surface 3; (b) late Miocene-Pliocene: PFBT developed, ES2 (blue) erosional surface 2 between U3 and U2; (c) mid-late Miocene: regional subsidence took place, U2 deposited (d) early Miocene: MBT and FHT developed; basal unconformity (purple) and ES1 (cyan): erosional surface 1 developed; (e) pre-Neogene: subsidence and formation of accommodation space, deposition of U1.

not only affected the growth of the prism near the subduction front but also affected the development of the backthrusts and pushed the FBTs more landward in the Aceh Basin, widening the accretionary wedge. The width of the wedge is about ~ 170 km in our study area and is about ~ 100 km in southern Sumatra (McNeill and Henstock, 2013, McNeill and Henstock, 2014), where the sediment supply is less. The development of the FBT was initiated in late Miocene-Pliocene period and continued until the recent time (Fig. 10), which is temporally coincident with an increased sediment supply in the Bengal and Nicobar fan area. Therefore, one can argue that the growth of the FBT in the fore-arc might have been influenced by the higher sediment supply in the Sumatran trench.

5.3. *Interaction among backthrusts, strike-slip faulting (WAF), and sedimentation*

In contrast with several previous studies (Chauhan, 2010; Martin

et al., 2014; Berglar et al., 2010) that documented the presence of either strike-slip or backthrust faulting in the area, our observations confirm the coexistence of both types of faulting at the seaward side of the Aceh Basin, in which the MBT and some paleo-FBTs are intersected by a strike-slip fault zone (Figs. 9 and 10). The major part of this fault assemblage consists of thrust faults (MBT and FBT), forming the north Sumatra backthrust system (NSBS) (Fig. 9). The recent FBT is active throughout the fore-arc in our study area. Although in most of the seismic images the MBT is mapped as a blind fault, we are not certain whether it is still active. Earlier studies (Martin et al., 2014; Berglar et al., 2010) suggested that the WAF developed as the result of slip partitioning in response to oblique plate convergence. However, the northern part of the Aceh Basin is very narrow where the GSF connects with the ANF, which might have led to the development of a trans-pressional regime in the fore-arc Aceh Basin in the south. Moreover, slightly different movements on WAF1 and WAF2 might have contributed in forming the depression observed between the northern and southern fore-arc highs at 5^0N (Fig. 9). However, this depression could also be linked with the passage of a high bathymetric feature on the downgoing plate (Singh et al., 2011b).

The growth of strike-slip faults in the accretionary wedge has been observed in an oblique subduction system. Along the Sumatran fore-arc high islands, a set of trench-subparallel strike-slip faults dissected the fore-arc high, and overprinted the older trench-parallel fold and thrust fault system (Samuel and Harbury, 1996). However, as detailed above it is clear that the backthrust system observed in the current fore-arc domain is very old compared to the strike-slip faults (WAF) and has played a central role in the development of the fore-arc. 3D sandbox modelling results indicate that backthrusts form a boundary between the accretionary wedge complex and fore-arc basin, even in a highly oblique subduction setting (McClay et al., 2004). Furthermore, these results show that strike-slip faults develop subsequently above the thrust faults rooted at the backstop. Therefore, contrary to the earlier observations that strike-slip fault plays as a crustal boundary separating the fore-arc basin and forearc high in oblique subduction system (e.g. Diament et al., 1992; Izart et al., 1994; Malod and Kamal, 1996; Martin et al., 2014), we suggest that despite the obliquity in a convergent margin, backthrust system is a major tectonic feature that marked the boundary between fore-arc basin and accretionary wedge complex.

The U3 sediments in Aceh Basin are mostly undeformed, which might be due to the development of a stress shadow in the basin linked with the presence of backthrusts, whereas the older units U2 and U1 are deformed. Byrne et al. (1993) reported that the trenchward edge of the fore-arc basin might experience some uplift, landward tilting and internal deformation with the growth of the accretionary wedge and uplift of the fore-arc high (Figs. 6 and 7). Such deformation of the sedimentary sequence trapped in the fore-arc basin might also be affected by the variation of the basal friction developed at the plate interface (Larroque et al., 1995), which balances the migration of the frontal thrusts near the trench and the backthrusts propagation through the wedge and onlapping pattern of the sedimentary deposits in the fore-arc basin (Noda, 2018) as evidenced in the Kumano fore-arc basin (Mannu et al., 2017).

Besides the current study, the importance of slip on backthrust in shaping the fore-arc domain is also observed farther south adjacent to the Nias and Simeulue Islands (Vita-Finzi, 2008) and in some other sections of the Sunda Arc (Silver and Reeds, 1988) including Java. The backthrust branches near the Simeulue Island are reported to be inactive at present (Singh et al., 2008). Furthermore, projection of relocated hypocenters of the 1976 event near the location of the 2004 earthquake in the northern Sumatran forearc suggests that the 1976 event may have initiated in the forearc basement as backthrust or a reactivated fault in the basement (Pesicek et al., 2010). A similar backthrust has also been observed in the Andaman region (Singh et al., 2013). Backthrusts have also been observed in other subduction margins, for instance in the Lesser Antilles (Torrini and Speed, 1989; Westbrook et al., 1988), southern Colombia (Meyer et al., 1976) and the Panama Trench (Silver et al., 1990).

6. Conclusions

Based on our observations using the high-resolution geophysical datasets we draw the following conclusions:

1) Major structural development associated with the northern Sumatra fore-arc domain took place in the Miocene. Both MBT and FHT were active in the early Miocene and took part in the uplift of the fore-arc high and eventually in the evolution of the Aceh Basin. Later on, the FBT started to become active from late Miocene onwards and the landward migration of the FBT might have been influenced by the very large sediment supply from eastern Himalaya in the Nicobar Fan. The identification of several phases of erosion in the sedimentary deposits implies that the fore-arc has experienced several phases of uplift. Further uplift over these highs may develop fore-arc islands in the future.
2) The FBT is active throughout the fore-arc in the study area but the MBT is imaged as a blind fault. A velocity low associated with the FBT suggests that the sediments associated with this fault zone are fluid saturated. Backthrusts (MBT and FBT) and a strike-slip fault zone (WAF) coexist at SW to the Aceh Basin below the north-eastern fore-arc slope. As the backthrusts are older, slip partitioning on the plane of FBT might have contributed in the development of the younger strike-slip fault.

Declaration of Competing Interest

The authors declare that they have no known competing financial interests or personal relationships that could have appeared to influence the work reported in this paper.

Acknowledgements

We are thankful to Western Geco for acquisition and processing of seismic reflection data and TGS for providing the high resolution MCS datasets. We are also thankful to IHS-Markit for providing us the free academic license for seismic interpretation. We acknowledged comments and suggestions from the reviewers that improved clarity of the manuscript. This study contributes to the IdEx Université de Paris ANR-18-IDEX-0001.

Appendix A. Supplementary material

Supplementary data to this article can be found online at https://doi.org/10.1016/j.jseaes.2021.104814.

References

Aubert, O., Droxier, A.W., 1996. Seismic stratigraphy and depositional signatures of the Maldives carbonate system (Indian ocean). Mar. Pet. Geol. 13, 503–536.
Beaudry, D., Moore, G.F., 1985. Seismic stratigraphy and Cenozoic evolution of West Sumatra fore-arc basin. The American Association of Petroleum Geologists Bulletin 69 (5), 742–759.
Berglar, K., Gaedicke, C., Franke, D., Ladage, S., Klingelhoefer, F., Djajadihardja, Y.S., 2010. Structural evolution and strike-slip tectonics off north-western Sumatra. Tectonophysics 480 (1-4), 119–132.
Bilham, R., England, P., 2001. Plateau "pop-up" in the great 1897 Assam earthquake. Nature 410 (6830), 806–809.
Byrne, D.E., Wang, W.-H., Davis, D.M., 1993. Mechanical role of backstops in the growth of fore arcs. Tectonics 12 (1), 123–144.
Chauhan, A.P.S., Singh, S.C., Hananto, N.D., Carton, H., Klingelhoefer, F., Dessa, J.-X., Permana, H., White, N.J., Graindorge, D., 2009. Seismic imaging of fore-arc back thrusts at northern Sumatra subduction zone. Geophys. J. Int. 179 (3), 1772–1780.
Chauhan, A.P.S., 2010. Structure of the Northern Sumatra subduction megathrust using seismic reflection and refraction data, Ph.D. Thesis, Institut de Physique du Globe de Paris, France.
Curray, J.R., 2005. Tectonics and history of the Andaman Sea region. J. Asian Earth Sci. 25 (1), 187–232.

Diament, M., Harjono H., Karta K., Deplus C., et al., 1992. Mentawai fault zone off Sumatra: A new key to the geodynamics of western Indonesia. Geology, 20, 259–262. 16, 25, 104, 175, 176.
Davis, D., Suppe, J., Dahlen, F.A., 1983. Mechanics of fold-and-thrust belts and accretionary wedges. J. Geophys. Res. 88 (B2), 1153. https://doi.org/10.1029/JB088iB02p01153.
Dickinson, W.R., Rich, E.I., 1972. Petrologic intervals and petrofacies in the Great Valley Sequence, Sacramento Valley, California. Geolog. Soc. America Bullet. 83 (10), 3007–3024. https://doi.org/10.1130/0016-7606(1972)83(3007:PIAPIT)2.0.CO;2.
Dickinson, W.R., 1995. Forearc basins. In: Busby, C.J., Ingersoll, R.V. (Eds.), Tectonics of Sedimentary Basins. Blackwell Science, Oxford, UK, pp. 221–261.
Fisher, D., Mosher, D.C., Austin, J.A., Gulick, S.P.S., Masterlark, T., Moran, K., 2007. Active deformation across the Sumatran fore-arc over the December 2004 Mw9.2 rupture. Geology 35, 99–102. https://doi.org/10.1130/G22993A.1.
Gahalaut, Vineet, et al., 2006. Constraints on 2004 Sumatra–Andaman earthquake rupture from GPS measurements in Andaman–Nicobar Islands. Earth Planet. Sci. Lett. 242.
Ghosal, D., Singh, S.C., Chauhan, A.P.S., Hananto, N.D., 2009. New insights on the Great Sumatra fault, NW offshore Sumatra, from marine data. AGU San Francisco T33B–T1917.
Ghosal, D., Singh, S.C., Chauhan, A.P.S., Hananto, N.D., 2012. New insights on the offshore extension of the Great Sumatran fault, NW Sumatra, from marine geophysical studies. Geochem. Geophys. Geosyst. 13 (11) https://doi.org/10.1029/2012GC004122.
Ghosal, D., Singh, S.C., Martin, J., 2014. Shallow subsurface morphotectonics of the NW Sumatra subduction system using an integrated seismic imaging technique. Geophy. Jour. Int. 198 (3), 1818–1831.
Grevemeyer, I., Flueh, E.R., Reichert, C., Bialas, J., Kläschen, D., Kopp, C., 2001. Crustal architecture and deep structure of the Ninetyeast Ridge hotspot trail from active-source ocean bottom seismology. Geophy. Jour. Int. 144 (2), 414–431. https://doi.org/10.1046/j.0956-540X.2000.01334.x.
Fowler, P., 1997. A comparative overview of prestack time migration methods: 67th Ann. Int. Soc. Explor. Geophys. Mtg., Soc. Expl. Geophys., Expanded Abstracts, 1571–1574.
Hall, R., 2012. Late Jurassic-Cenozoic reconstructions of the Indonesian region and the Indian Ocean. Tectonophysics 570-571, 1–41.
Izart, A., Mustafa, K.B., Malod, J.A., 1994. Seismic stratigraphy and subsidence evolution of the Northwest Sumatra fore-arc basin. Mar. Geol. 122 (1–2), 109–124. https://doi.org/10.1016/0025-3227(94)90207-0.
Karig, D. E., Suparka S., Moore G. F., Hehanussa P. E., 1979. Structure and Cenozoic evolution of the Sunda Fore-arc in the Central Sumatra region, in Geological and Geophysical Investigation of Continental Margin, edited by J. S. Watkins, L. Montadert, and P. Wood-Dickerson, AAPG Memoir, 29, 223–237.
Kopp, H., Fleueh E.R., Klaeschen D., Bialas J., Reichert C., 2001. Crustal structure of the central Sumatra margin at the onset of oblique subduction, Geophy. Jour. Int., 147.
Kopp, H., Kukowski N., 2003. Backstop geometry and accretionary mechanics of the Sunda margin, Tectonics, 22.
Larroque, C., Calassou, S., Malavielle, J., Chanier, F., 1995. Experimental modelling of forearc basin development during accretionary wedge growth. Basin Res. 7 (3), 255–268.
Lee, T.-Y., Lawver, L.A., 1995. Cenozoic plate reconstruction of Southeast Asia. Tectonophysics 251 (1-4), 85–138.
Lee, T.Y., Lawver, L.A., 1995. Cenozoic plate reconstruction of Southeast Asia. Tectonophysics. https://doi.org/10.1016/0040-1951(95)00023-2.
Lewis K. B., Petinga J. R., 1993. The emerging, imbricate frontal wedge of the Hikurangi Margin. In: South Pacific Sedimentary Basins, Sedimentary Basins of the World 2 (Ed. by P. F. Ballance), pp.225-250. Elsevier Science Publisher.
Lüschen, E., Müller, C., Kopp, H., Engels, M., Lutz, R., Planert, L., Shulgin, A., Djajadihardja, Y.S., 2011. Structure, evolution and tectonic activity of the eastern Sunda forearc Indonesia, from marine seismic investigations. Tectonophysics 508 (1-4), 6–21.
Malod, J.A., Kamal B. M., 1996. The Sumatran margin: oblique subduction and lateral displacement of the accretioanry prism, Geol. Soc. London, Sp. Publications, 106.
Mannu, U., Ueda, K., Willett, S.D., Gerya, T.V., Strasser, M., 2017. Stratigraphic signatures of forearc basin formation mechanisms. Geochem. Geophys. Geosyst. 18 (6), 2388–2410. https://doi.org/10.1002/ggge.v18.610.1002/2017GC006810.
Marcaillou, B., Collot, J.-Y., 2008. Chronostratigraphy and tectonic deformation of the North Ecuadorian-South Colombian offshore Manglares forearc basin. Mar. Geol. 255 (1-2), 30–44.
Martin, K.M., Gulick, S.P.S., Bangs, N.L.B., Moore, G.F., Ashi, J., Park, J.-O., Kuramoto, S., Taira, A., 2010. Possible strain partitioning structure between the Kumano fore-arc basin and the slope of the Nankai Trough accretionary prism. Geochem. Geophys. Geosyst. 11 (5) https://doi.org/10.1029/2009GC002668.
Martin, J., Ozbek A., Combee L., Lunde N., Bittleston S., Kragh E., 2000. Acquisition of marine point receiver seismic data with a towed streamer, SEG, Expanded abstract.
Martin, K., Gulick, S.P.S., Austin, J.A., Bergler, K., Franke, D., 2014. The West Andaman Fault: A complex strain-partitioning boundary at the seaward edge of the Aceh Basin, offshore Sumatra. Tectonics 33 (5), 786–806.
McClay, K.R., Whitehouse, P.S., Dooley, T., Richards, M., 2004. 3D evolution of fold and thrust belts formed by oblique convergence. Mar. Pet. Geol. 21, 857–877. https://doi.org/10.1016/j.marpetgeo.2004. 03.009.
McNeill, L.C., Henstock, T.J., 2014. Fore-arc structure and morphology along the SumatraAndaman subduction zone. Tectonics 33 (2), 112–134.
McNeill, L.C., Henstock, T.J., 2014. Forearc structure and morphology along the Sumatra-Andaman subduction zone. Tectonics 33 (2), 112–134. https://doi.org/10.1002/2012TC003264.
McNeill, L.C., Dugan, B., Backman, J., Pickering, K.T., Pouderoux, H.F.A., Henstock, T.J., Petronotis, K.E., Carter, A., Chemale, F., Milliken, K.L., Kutterolf, S., Mukoyoshi, H., Chen, W., Kachovich, S., Mitchison, F.L., Bourlange, S., Colson, T.A., Frederik, M.C. G., Guèrin, G., Hamahashi, M., House, B.M., Hüpers, A., Jeppson, T.N., Kenigsberg, A.R., Kuranaga, M., Nair, N., Owari, S., Shan, Y., Song, I., Torres, M.E., Vannucchi, P., Vrolijk, P.J., Yang, T., Zhao, X., Thomas, E., 2017. Understanding Himalayan erosion and the significance of the Nicobar Fan, Earth Panet. Sci. Lett. 475, 134–142.
Moeremans, R., Singh, S.C., 2014. Seismic evidence of continental margin origin for the northern segment of the Ninety-East Ridge in the Bay of Bengal. Geophys. Res. Lett. 341 https://doi.org/10.1002/2014GL061598.
Moore, J.C., Silver, A., 1987. Continental margin tectonics: Submarine accretionary prisms. Rev. Geophys. https://doi.org/10.1029/RG025i006p01305.
Moser, T.J., 1991. Shortest path calculation of seismic rays. Geophysics 56 (1), 59–67.
Mosher, D.C., Austin, J.A., Fisher, D., Gulick, S.P.S., 2008. Deformation of the northern Sumatra accretionary prism from high-resolution seismic reflection profiles and ROV observations. Mar. Geol. 252 (3-4), 89–99. https://doi.org/10.1016/j.margeo.2008.03.014.
Mukti, M.M., 2013. Tectonic evolution of the South Sumatra-Java forearc system from deep seismic reflection data, PhD thesis, Institut de Physique du Globe de Paris, France.
Mukti, M., Singh, S.C., Hananto, N.D., Deighton, I., Moeremans, R., Permana, H., 2012. Structural evolution of backthrusting in the Mentawai Fault Zone, offshore Sumatra fore-arc. Geochem. Geophy. Geosys. 13 https://doi.org/10.1029/2012GC004199.
Najman, Y., Bracciali, L., Parrish, R.R., Chisty, E., Copley, A., 2016. Evolving strain partitioning in the Eastern Himalaya: the growth of the Shillong Plateau, Earth Planet. Sci. Lett. 433, 1–9.
Noda, A., 2018. Forearc basin stratigraphy and interactions with accretionary wedge growth according to the critical taper concept. Tectonics 37 (3), 965–988.
Pesicek, J.D., Thurber, C.H., Zhang, H., DeShon, H.R., Engdahl, E.R., Widiyantoro, S., 2010. Teleseismic double-difference relocation of earthquakes along the Sumatra-Andaman subduction zone using a 3-D model. J. Geophys. Res. Solid Earth 115 (B10303), 1–20.
Ryan, H.F., Scholl, D.W., 1989. The evolution of forearc structures along oblique convergent margin, central Aleutian arc. Tectonics 8, 497–516.
Samuel, M.A., Harbury, N.A., 1996. The Mentawai fault zone and deformation of the Sumatran forearc in the Nias area. In: Tectonic Evolution of Southeast Asia (edited by Hall R. and Blundell D.). Geological Society of London Special Publication, 106.
Samuel, M.A., Harbury, N.A., Bakri, A., Banner, F.T., Hartono, L., 1997. A new stratigraphy for the islands of the Sumatran Fore-arc, Indonesia. Jour. Asian Earth Sci. 15 (4-5), 339–380.
Schlüter, H.C., et al., 2002. The Makran accretionary wedge: Sediment thicknesses and ages and the origin of mud volcanoes. Mar. Geol. 185 https://doi.org/10.1016/S0025-3227(02)00192-5.
Sieh, K., Natawidjaja, D., 2000. Neotectonic of the Sumatran fault Indonesia. J. Geophys. Res. 105, 28295–28326. https://doi.org/10.1029/2000JB900120.
Silver, E. A., Reed D. L., 1988. Backthrusting in accretionary wedges, Jour. Geophy. Res., 93.
Silver, E.A., Reed, D.L., Tagudin, J.E., Heil, D.J., 1990. Implications of the north and south Panama thrust belts for the origin of the Panama orocline. Tectonics 9 (2), 261–281.
Singh, S.C., Carton, H., Tapponier, P., Hananto, N., Chauhan, A.P.S., Hartoyo, D., Bayly, M., Moeljopranoto, S., Bunting, T., Christie, P., Lubis, H., Martin, J., 2008. Seismic evidence for broken oceanic crust in the 2004 Sumatra earthquake epicentral region. Nat. Geosci. 1, 771–781.
Singh, S. C., Hananto, N. D., Chauhan, A. P. S., 2011b. Enhanced reflectivity of back thrusts in the recent great Sumatran earthquake rupture zones, Geophys. Res. Lett., 38, doi:10.1029/2010GL046227.
Singh, S.C., Hananto, N., et al., 2011b. Aseismic zone and earthquake segmentation associated with a deep subducted seamount in Sumatra. Nat. Geosci. 4, 308–311.
Singh, S.C., Chauhan, A.P.S., Calvert, A.J., Hananto, N.D., Ghosal, D., Rai, A., Carton, H., 2012. Seismic evidence of bending and unbending of subducting oceanic crust and the presence of mantle megathrust in the 2004 Great Sumatra earthquake rupture zone, Earth Planet. Sci. Lett. 321–322, 166–176. https://doi.org/10.1016/j.epsl.2012.01.012.
Singh, S.C., Moeremans, R., McArdle, J.o., Johansen, K., 2013. Seismic images of the sliver strike-slip fault and backthrust in the Andaman-Nicobar region. J. Geophys. Res. Solid Earth 118 (10), 5208–5224.
Singh, S. C., Moeremans, R., 2017. Chapter 13 Anatomy of the Andaman–Nicobar subduction system from seismic reflection data. Geological Society, London, Memoirs, 47(1), 193–204. https://doi.org/10.1144/m47.13.
Scales, J.A., 1987. Tomographic inversion via the conjugate inversion method. Geophysics 52, 179–185.
Torrini, R., Speed, R.C., Mattioli, G.S., 1985. Tectonic relationships between forearc-basin strata and the ac- cretionary complex at Bath. Barbados. Bull. Geol. Sor. Am. 96 (7), 861. https://doi.org/10.1130/0016-7606(1985)96<861:TRBFSA>2.0.CO;210.1130/8524.
Torrini, R., Speed, R.C., 1989. Tectonic wedging in the fore-arc basin accretionary prism transition, Lesser Antilles fore-arc. J. Geophys. Res. 94 (B8), 10549–10584.
Van Avendonk, H.J.A., Shillington, D., Holbrook, W.S., Hornbach, M., 2004. Infering crustal structure in the Aleutian island arc from a sparse wide-angle seismic data set. Geochem. Geophys. Geosyst. 5 (8), 1527–2087.

Vita-Finzi, C., 2008. Neotectonics and the 2004 and 2005 earthquake sequences at Sumatra, Marine Geology, 248.

Westbrook, G.K., Ladd, J.W., Buhl, P., Bangs, N., Tiley, G.J., 1988. Cross section of an accretionary wedge: Barbados ridge complex. Geology 16 (7), 631. https://doi.org/10.1130/0091-7613(1988)016<0631:CSOAAW>2.3.CO;2.

Willett, S., Beaumont, C., Fullsack, P., 1993. Mechanical model for the tectonis of doubly vergent compressional orogen. Geology 21, 371–374.